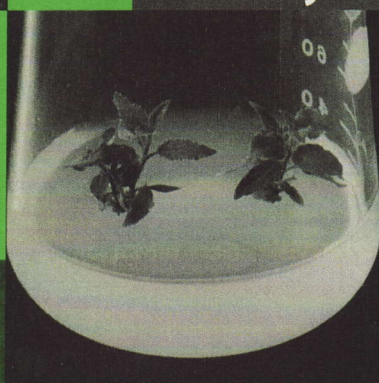


K. Omasa • H. Saji
S. Youssefian • N. Kondo (Eds.)

Air Pollution and Plant Biotechnology

Prospects for Phytomonitoring
and Phytoremediation



Springer

18

Diagnosis of Stomatal Response and Gas Exchange of Trees by Thermal Remote Sensing

Kenji Omasa

Department of Biological and Environment Engineering, Graduate School of Agricultural and Life Sciences, The University of Tokyo, Yayoi 1-1-1, Bunkyo-ku, Tokyo 113-8657, Japan

1. Introduction

Air pollution and meteorological changes have influenced the health of trees growing in urban and forest areas (Guderian 1985; Sakai and Larcher 1987; Schulze et al. 1989; Omasa et al. 1996; Sandermann et al. 1997; Paoletti 1998; Waring and Running 1998). Acid rain and acid fog are among the factors considered to have such an effect (Cowling 1989; Schulze et al. 1989). The first abnormal symptoms to appear are stomatal closure and decrease in photosynthesis and growth. When the injury is severe, the symptoms extend to visible injury of leaves and withering. Withered branches are often observed in polluted urban areas. In recent years a forest decline, which may possibly be due to acid rain and acid fog as well as other air pollutants and meteorological changes, has been reported in Europe, North America, and East Asia (Guderian 1985; Cowling 1989; Schulze et al. 1989; Environment Agency of Japan 1991-1993, Sandermann et al. 1997; Paoletti 1998).

The development of remote sensing from satellites and airplanes has proved important for monitoring the effects (Colwell 1983; Rencz 1999). Color infrared photographs and multispectral data taken from an airplane have often been used to estimate the visible injury of trees and forest decline. Global changes in forests have been observed by satellite remote sensing such as LANDSAT/TM,

Air Pollution and Plant Biotechnology
—Prospects for Phytomonitoring and Phytoremediation—
Edited by K. Omasa, H. Saji, S. Youssefian, and N. Kondo
© Springer-Verlag Tokyo 2002

SPOT/HRV, NOAA/AVHRR, and EOS/MODIS. For example, the LANDSAT/TM provides several spectral images with a high resolution of 30 m in the visible to near-infrared range and 120 m in the thermal infrared range. Therefore, these images have been used for analyses of decline and evapotranspiration in urban woods and local areas of forests (Colwell 1983; Nemani and Running 1989; Hobbs and Mooney 1990). A recent technical trend in remote sensing from airplanes and satellites is hyperspectral observation capable of resolving from several tens to several hundreds of spectral bands (Hobbs and Mooney 1990; Rencz 1999; Omasa, 2000). Hyperspectral analysis in the visible to near-infrared region may be able to provide more phytobiological information on changes in contents of water and biochemical components in living plants and soils, productivity and stresses of individual plants and vegetation, and classification of plant species.

Meanwhile, portable thermal cameras (thermographic system) have often been used to remotely measure changes in temperature of plants and canopy as a surrogate for stomatal conductance ($=1/\text{stomatal resistance}$) and photosynthesis rate (Schurer 1975; Omasa et al. 1979, 1990, 1993; Omasa 1994; Horler et al. 1980; Hashimoto et al. 1984, 1990; Inoue et al. 1990; Taconet et al. 1995; Jones 1999). In the latter half of the 1970s, thermal camera joined with a computer was developed for image analysis of leaf temperature (Omasa et al. 1979; Hashimoto et al. 1984). Consequently, Omasa et al. (1981a-c; Omasa and Croxdale 1992) quantitatively evaluated spatial distributions of stomatal resistance ($=1/\text{stomatal conductance}$), transpiration rate, and absorption rate of air pollutants all over the attached leaf from leaf temperature. Recently, such quantitative study has been noticed in thermal image sensing although it is difficult to analyze quantitatively energy balance over the leaf surface (Jones 1999). The microthermogram provided information on responses of stomata at sites between veins of rice plants (Omasa 1996).

It is also very difficult to spatially evaluate stomatal resistance and transpiration rate of plants growing in the field. However, the thermal image can provide information for early detection of plant stresses, because stomatal closure occurs before the appearance of visible injury, and for screening of plants with high growth and high air pollutant absorption under steady-state thermal environments (Omasa and Aiga 1987; Omasa 1990a, 1994). Helicopter-borne remote sensing by a thermal camera was effective for early detection of environmental stress of woody canopy (Omasa et al. 1993; Omasa 1994).

2. Information Obtained from Leaf Temperature

Water evaporates from mesophyll and epidermal cell walls in the substomatal cavity and diffuses into the atmosphere through the stomata and boundary layers of leaves and trees. Carbon dioxide (CO_2), for photosynthesis, and air pollutants enter the leaf in the opposite direction to that of the water vapor (Monteith 1973;

Omasa 1979; Jones 1992). A simple resistance model for heat and gas exchange between a tree and free air is shown in Fig.1. Resistance in transfer between the gas-liquid interface in the substomatal cavity and air on the leaf is represented as the bulk stomatal resistance. Resistance between the leaf boundary layer and free air is expressed as the aerodynamic resistance. Although the bulk stomatal resistance indicates stomatal opening, it also depends on the number of stomata, their size and structure. The aerodynamic resistance varies with wind velocity, atmospheric stability, leaf shape, and the spatial structure of trees.

When the leaf surface is not wet with rain or dew, the transpiration rate, W , which is the flux in diffusion of water vapor from the leaf to free air, is given by

$$W = \{X_s(T_1) - \Phi X_s(T_a)\} / (r_{aw} + r_{sw}) \quad (1)$$

where T_1 is the leaf temperature, T_a is the air temperature, $X_s(T)$ is the saturated water vapor diffusion at temperature T , Φ is the relative humidity, r_{aw} is the

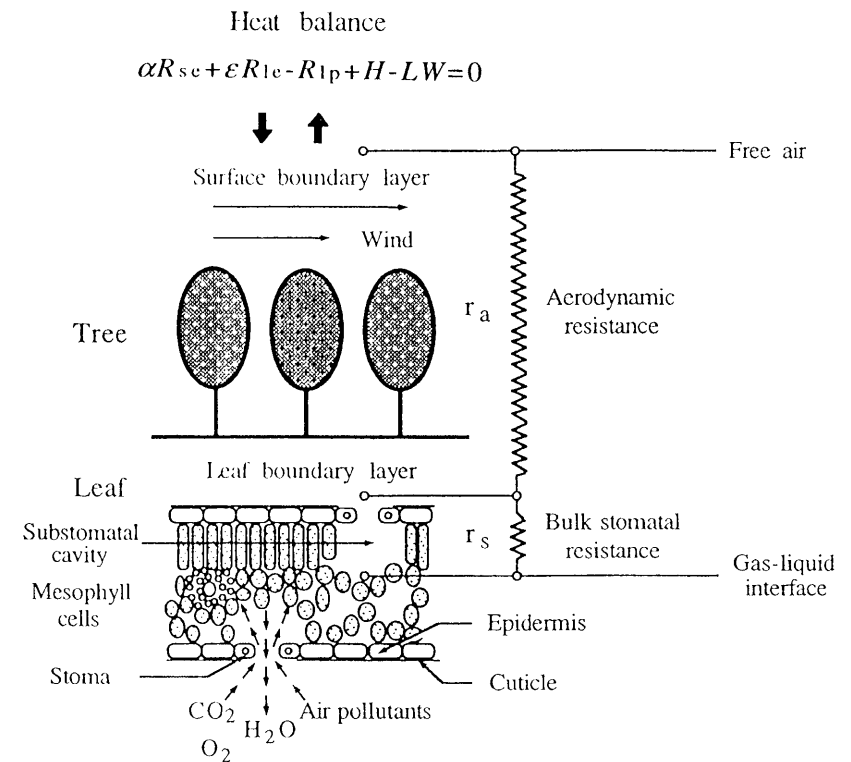


Fig. 1. Simple resistance model for heat and gas exchange between tree and its environment

aerodynamic resistance to water vapor diffusion, and r_{sw} is the bulk stomatal resistance to water vapor diffusion.

The absorption rate of gases such as CO₂ and air pollutants, Q is

$$Q=(C_a-C_1)/(r_{ag}+r_{sg}) \quad (2)$$

where C_a is the gas concentration of free air, C_1 is the gas concentration at the gas-liquid interface in the stomatal cavity, r_{ag} is the aerodynamic resistance to gas diffusion, and r_{sg} is the bulk stomatal resistance to gas diffusion. The C_1 of major air pollutants such as SO₂, NO₂, O₃, and formaldehyde in the healthy leaves can be assumed nearly to equal 0 $\mu\text{l l}^{-1}$ (ppmv) because the metabolic rate in the tissues is very rapid (see Omasa et al., this volume). However, the C_1 of CO₂ dependent on photosynthesis and respiration and of most organic air pollutants varies according to species and growth conditions (Jones 1992; see Omasa et al., this volume).

On the other hand, the heat balance at the leaf surfaces is given by

$$\alpha R_{sc} + \varepsilon R_{lc} - R_{lp} + H - LW = 0 \quad (3)$$

where R_{sc} is the short-wavelength radiation ($\leq 3 \mu\text{m}$) from the environment, α is the absorption coefficient of short-wavelength radiation of the leaf, R_{lc} is the long-wavelength radiation ($> 3 \mu\text{m}$) from the environment, ε is the emissivity of long-wavelength radiation of the leaf, R_{lp} is the long-wavelength radiation from the leaf surface, H is the sensible heat transfer by convection, and L is the latent heat of vaporization.

According to Planck's law, R_{lp} in Eq. 3 is

$$R_{lp} = \varepsilon \sigma T_1^4 \quad (4)$$

and H is

$$H = \rho c_p (T_a - T_1) / r_{ak} \quad (5)$$

where σ is the Stefan-Boltzmann constant, ρc_p is the volumetric heat capacity of the air, and r_{ak} is the aerodynamic resistance to heat transfer.

Substituting Eqs. 4 and 5 in Eq. 3 gives the following equation for transpiration rate, W :

$$W = \{ \alpha R_{sc} + \varepsilon (R_{lc} - \sigma T_1^4) + \rho c_p (T_a - T_1) / r_{ak} \} / L \quad (6)$$

In the range of growth temperature of trees, R_{lp} is approximated by

$$R_{lp} = \varepsilon \sigma (A_0 T_1 + B_0) \quad (7)$$

and W is expressed as a simplified equation

$$W = AT_1 + B \quad (8)$$

where

$$A = -(\varepsilon \sigma A_0 + \rho c_p / r_{ak}) / L \quad (9)$$

$$B = (\alpha R_{sc} + \varepsilon (R_{lc} - \sigma B_0) + \rho c_p T_a / r_{ak}) / L \quad (10)$$

and A_0 is $1.06 \times 10^8 \text{ K}^3$ and B_0 is $-2.37 \times 10^{10} \text{ K}^4$ in the range of 293.15 to 303.15 K (20° to 30°C).

Values for the micrometeorological parameters of outdoor trees in Eqs. 9 and 10 change with time and situation. When there is cloud and a breeze, thermal conditions such as air temperature, humidity, radiation and air current are maintained relatively constant and uniform. The poor effect of direct solar radiation and the shade of trees on the parameters also decreases under a cloudy sky. Therefore, A and B in Eqs. 9 and 10 are assumed to be constant values under such thermal conditions, and W in Eq. 8 is expressed as a linear function of T_1 . Because the increase in T_1 means a decrease of W in the equation, the leaf temperature may be used as an indicator of tree health and activity.

The relationship between aerodynamic resistances in heat and mass transfer is approximated by

$$r_{ak} = r_{aw} = r_{ag} \quad (11)$$

except under the conditions of stable atmosphere in the night. The bulk stomatal resistance of gas is related to that of water vapor by

$$r_{sg} = (D_w / D_g) r_{sw} \quad (12)$$

where D_w is air-water vapor diffusivity and D_g is air-gas vapor diffusivity. The bulk stomatal resistance, r_{sw} , is transformed into the following equation by substituting Eqs. 8 and 11 in Eq. 1.

$$r_{sw} = \{ X_s(T_1) - \Phi X_s(T_a) \} / (AT_1 + B) - r_{ak} \quad (13)$$

Equation 13 shows that the leaf temperature T_1 gives information about r_{sw} , an indicator of stomatal opening, under constant thermal conditions. The stomatal conductance, which is often obtained for the measurement using a diffusion porometer, is given by $1/r_{ws}$.

Equation 2 is transformed into the following equation by substituting Eqs. 11 and 12:

$$Q = (C_a - C_1) / \{ r_{ak} + (D_w / D_g) r_{sw} \} \quad (14)$$

When the gas concentration C_1 at the gas-liquid interface in the stomatal cavity is known, information about the absorption rate Q of gases is also obtained from T_1 .

3. Image Instrumentation of Leaf Temperature

3.1 Portable Thermal Camera

Portable thermal cameras of both optical-mechanical scanning and electric scanning types (focal plane array sensor) are on the market. The thermal camera of the optical-mechanical scanning type with an InSb (3 to 5 μm) or HgCdTe (8 to 13 μm) detector cooled by liquid nitrogen (77 K) or Stirling cryocooler has been used for a long time. The spectral range of 3 to 5 μm is not suitable for measuring the leaf temperature of trees outdoors owing to the direct effect of the sun's radiation. Consequently, a thermal camera with HgCdTe detector of 8 to 13 μm range has been generally used for field observation. Figure 2A shows a portable thermal camera (JEOL, JTG-5200) with an optical-mechanical scanning type of mirror vibration and a HgCdTe detector (8 to 13 μm , cooled by liquid nitrogen). This camera needs a frame time of more than 0.1 s. The signals detected by the camera head are converted into 16-bit digital signals (512Hx480V) and analyzed by an image processor with camera control functions. A series of thermal images is measured continuously by the system and stored in a builtin hard disk and MO disks. In outdoor situations, it is possible to carry out simple analyses of the image data using the image processor. This system gives a sensitivity (black body at 30°C) of 0.05°C and a horizontal resolution of 420 lines. The temperature-resolving power is improved to about 0.01°C by averaging the images. Measurement accuracy such as uniformity and repeatability of temperature is below 1% or 0.5°C, whichever is greater.

The recent advance in the development of thermal array sensors is remarkable. A smaller-sized, convenient thermal camera with a frame rate of 30 Hz, similar to a CCD video camera, is realized by development of new focal plane array (FPA) technology such as a 320x240 uncooled FPA (8 to 14 μm) with a sensitivity of 0.1°C and a measurement accuracy of $\pm 2\%$ or 2°C, whichever is greater (Avio, TVS-610) (Fig.2B). However, the measurement accuracy of an uncooled FPA has been inferior to that of the optical-mechanical scanning type until now.

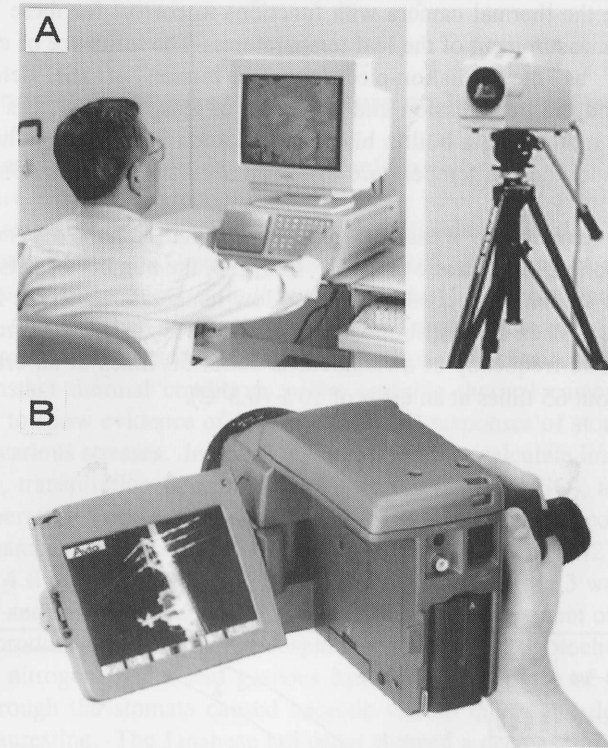


Fig. 2A, B. Portable thermal cameras of optical-mechanical scanning type (A, JEOL, JTG-5200) and uncooled FPA type (B, Avio, TVS-610)

3.2 Accuracy in Measuring Leaf Temperature

For a perfectly diffuse and opaque leaf surface, thermal radiation $R_p(T, T_s)$ from the surface of temperature T in the spectral sensitivity range of the thermal camera is given by

$$R_p(T, T_s) = \varepsilon_p R_b(T) + (1 - \varepsilon_p) R_c(T_s) \quad (15)$$

where ε_p is the emissivity of the leaf surface in the spectral range, $R_b(T)$ is the spectral radiation from the black body of temperature T , and $R_c(T_s)$ is the spectral radiation from the environment of temperature T_s to the leaf surface. The emissivity ε_p of the leaf in the spectral range 8 to 13 μm is 0.95 to 0.99 (Gates et al. 1965; Fuchs and Tanner 1966; Omasa et al. 1979). The measured temperature

is affected by the emissivity and radiation from the environment. Therefore, it is necessary to use the thermal camera with functions to correct for these factors to obtain an exact measurement of the leaf temperature. The influence of changes in functions, such as the radiation-electricity conversion of the detector, its amplification, and the transmission and reflection of lens, filter, etc., is corrected continuously by monitoring a built-in black body source in the camera head. It is possible to measure the leaf temperature within an accuracy of 0.1 K (Omasa et al. 1979).

The error in temperature measured with the thermal camera depends on the spatial distribution of temperature (Fig. 3). In Fig. 3, the number of slits indicates the frequency of switchover between high and low temperatures on the horizontal line of the image. When the distribution of temperature is zigzag, the error reaches its maximum. The frequency of switchover is about 50 times at an error of 5% (0.25°C) and about 65 times at an error of 10% (0.5°C).

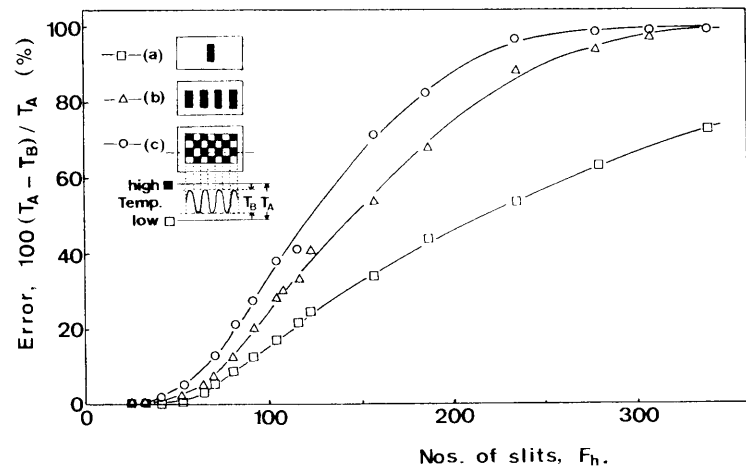


Fig. 3. Relationship between the error in temperature measured with the thermal camera (JEOL, JTG-5200) and the change in spatial distribution of temperature (from Omasa et al. 1993). The black and white patterns made by slits (a) to (c) show the difference in spatial distribution of temperature where the black area is high temperature and the white area is low temperature, T_A ($\approx 5^\circ\text{C}$) is the difference in real temperature between black and white areas, and T_B is that in measured temperature. The number of slits means frequency of switchover at high and low temperatures on a horizontal line of the image

4. Diagnosis of Trees by Leaf Temperature Image

4.1 Diagnosis of Effects of O_3 Exposure on Trees

Abiotic and biotic stresses such as air pollutants, water deficit, high and low temperature, and virus infection cause spatially heterogeneous impairment of the attached leaves (Omasa et al. 1981b, c, 1987; Hashimoto et al. 1984; Daley et al. 1989; Omasa 1990a, b; Omasa and Croxdale 1992; Osmond et al. 1998). Such heterogeneous impairment is indicated in stomatal response and photosynthetic activity. As described in Section 2, the leaf temperature provides information about stomatal response, transpiration and absorption of air pollutants and CO_2 under constant thermal conditions. The portable thermal camera can be used, therefore, to show evidence of spatially different responses of stomata in attached leaves to various stresses. In addition, it is possible to calculate images of stomatal resistance, transpiration rate, and absorption rate of NO_2 , SO_2 , and O_3 from the leaf temperature image measured under controlled thermal conditions in the growth chamber (Omasa et al. 1981a-c; Omasa and Croxdale 1992).

Figure 4 shows the effects of $0.1 \mu\text{l l}^{-1}$ O_3 exposure during 3 weeks on Chinese laurestine and Japanese red cedar. Ozone is a major component of photochemical oxidants produced in the urban atmosphere by a series of photochemical reactions involving nitrogen oxides and gaseous hydrocarbons. Entry of O_3 into the leaf tissues through the stomata caused necrotic visible injury and defoliation to the Chinese laurestine. The Japanese red cedar showed a decrease in growth rate, but there was no visible injury. The leaf temperature in both trees increased with exposure time because of stomatal closure and death of the leaves (only Chinese laurestine). This temperature rise in the Japanese red cedar appeared especially in the upper part of the tree. It is difficult to measure spatial differences in the response of stomata of trees with attached needle leaves to environmental stimuli using ordinary porometers. However, use of the portable thermal camera makes it possible to obtain such spatial information easily.

4.2 Diagnosis of Street Trees

Street trees in urban areas grow under severe environmental conditions. The trees are exposed continuously to harmful gas from car exhausts and other air pollutants. Buildings interrupt sunlight falling on the trees, and street lamps illuminate them at night. Because the paved roads obstruct rainwater permeating into the soil together with a supply of nutrients from dead leaves, the soil water content, soil nutrients, and humidity decrease in urban areas. The effect first shows as a decrease in transpiration and photosynthesis. Although porometers and micrometeorological methods are used for measuring rates of transpiration and photosynthesis, these cannot provide the spatial distribution of these processes in

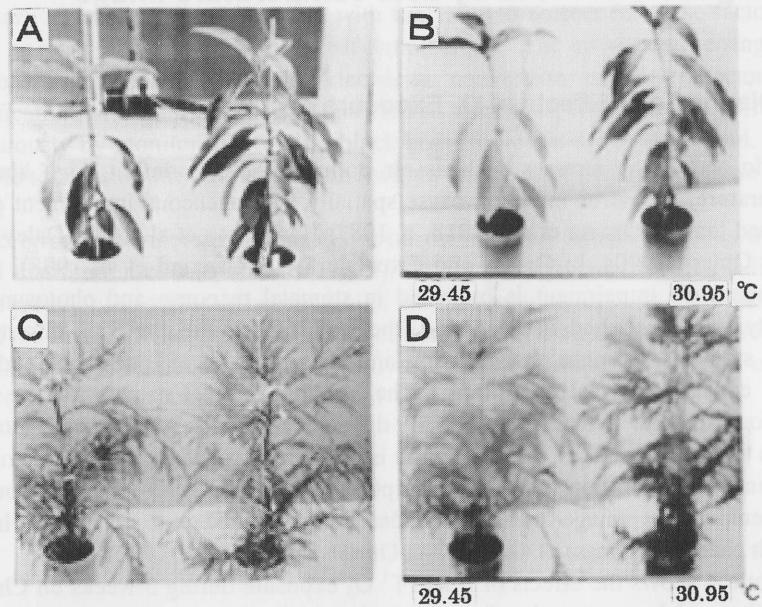


Fig. 4A-D. Effects of O_3 exposure on trees (from Shimizu et al. 1993). **A** Photograph of Chinese laurestine (*Viburnum odoratissimum* Ker-Gawler var. awabuki (K.Koch) Zabel), **B** Thermal image of the Chinese laurestine, **C** Photograph of Japanese red cedar (*Cryptomeria japonica* (L.fil.) D.Don), **D** Thermal image of the Japanese red cedar. The injured tree on the left side in the photograph and in the thermal image was exposed to $0.1 \mu l l^{-1} O_3$ for 3 weeks under $25^\circ C$, 70%RH, and $200-400 \mu mol photons m^{-2} s^{-1}$. The healthy tree on the right side was grown under the same conditions without O_3 exposure. The *gray scale* on the underside in the thermal image represents the temperature scale. The temperature shown by *white* is higher than that shown by the *black*

leaves and branches.

Figure 5 shows a photograph and a thermal image of zelkova trees growing in an urban street. The thermal image was measured under cloudy and breezy conditions. The leaf temperature of the tree on the left (*a* in Fig.5A and 5B) was higher than on the right (*b*) and other trees; this indicates stomatal closure and decrease in transpiration and photosynthesis in the tree on the left. These phenomena might be caused by volatile matter from a gasoline service station on the left-hand side. The tree on the right (*b*) was healthy owing to a sufficient supply of light, nutrients, and water from vacant land on the right-hand side. Although growth of the tree on the left (*a*) was poorer than that of the tree on the right, leaf injury was not visible. The combined use of the thermal camera and the porometer thus makes it possible to diagnose the health of trees precisely.

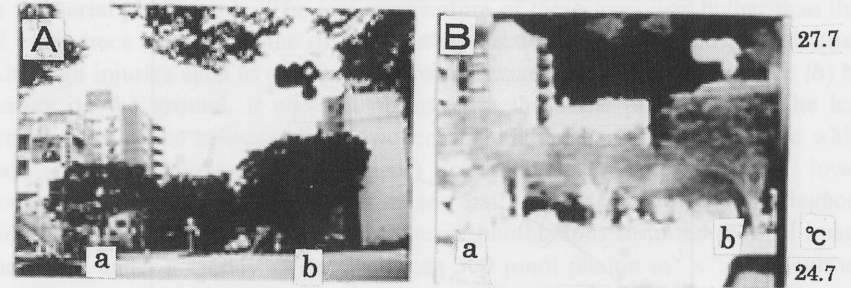


Fig. 5A, B. Photograph (**A**) and thermal image (**B**) of zelkova (*Zelkova serrata* (Thunb.) Makino) trees growing in an urban street (Omasa et al. 1990). Environmental conditions: air temperature, $26.5^\circ C$; light intensity, about $500 \mu mol photon m^{-2} s^{-1}$

Figure 6 shows the relationship between stomatal conductance and photosynthetic photon flux density (PPFD) for some species of healthy trees. These data were measured from 1300 to 1800h. The lowered PPFD tended to decrease stomatal conductance irrespective of species, although the data vary with each leaf site. In particular, stomatal conductance decreased rapidly below $200 \mu mol photon m^{-2} s^{-1}$. However, the rate of decrease was low above $300 \mu mol photon m^{-2} s^{-1}$ and reached different steady-state conditions in each species. Stomatal conductance is a reciprocal of stomatal resistance and an indicator of stomatal opening. Therefore, the decrease of stomatal conductance shown in Fig.6 indicates stomatal closure and a decrease in the rates of transpiration and photosynthesis. The stomata of healthy leaves opened rapidly after sunrise and closed slowly in the afternoon. The stomata of injured and water-stressed leaves did not open properly in the daytime. When it was cloudy, the PPFD was below $500 \mu mol photon m^{-2} s^{-1}$. Therefore, the thermal image used for diagnosis should be measured under a cloudy sky with PPFD of 300 to $500 \mu mol photon m^{-2} s^{-1}$. The effects of stomatal closure caused by water stress in the daytime are avoided by measurements under such conditions.

4.3 Diagnosis of Trees from a Helicopter

Woods and forests in urban areas and the neighboring mountains have been injured by the various environmental changes just described. However, it is difficult to diagnose damage to individual trees throughout the woods and forests by means of measurements made on the ground. Recently, thermal remote sensing from satellites and airplanes has been shown to estimate the function of woods and forests (Hobbs and Moony 1990; Omasa et al. 1993). Because helicopters can

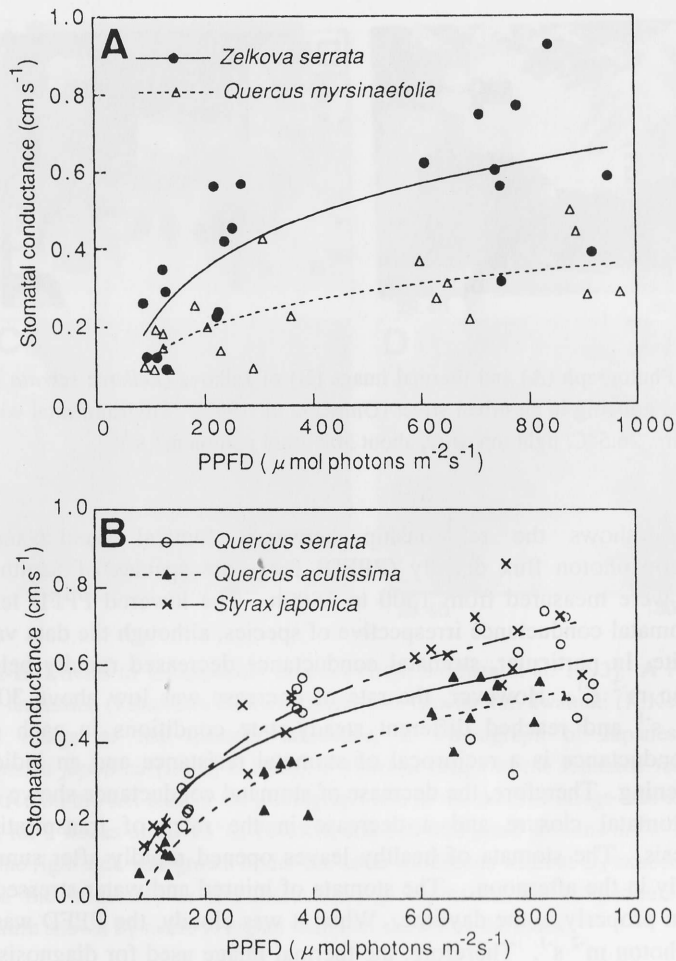


Fig. 6A, B. Relationship between stomatal conductance and photosynthetic photon flux density (PPFD) for some species of healthy tree (Omasa et al. 1993). Environmental conditions: air temperature, 30°-33°C; relative humidity, 50%-60%

approach a height of only several tens of meters, remote sensing from a helicopter makes it possible to diagnose individual trees (Omasa et al. 1993).

Figure 7 shows an aerial photograph and a thermal image of temple woods and the adjacent area in the suburbs of Tokyo. These were measured by the portable thermal camera from a helicopter at a height of about 300 m under cloudy and breezy conditions. In the temple woods, Japanese red pines (*Pinus densiflora* Sieb. et Zucc.) (a in Figs. 7A and 7B) were standing almost dead and many

Japanese red cedars had died back at their tops. These injuries were also observed in the aerial photograph. The leaf temperature of these trees was higher than that of other trees because of the decrease in stomatal conductance and transpiration. Although injuries such as abnormal leaf shape were found in a zelkova tree (b) by survey on the ground, it was not observed in the aerial photograph. The leaf temperature of the zelkova tree, however, was higher than that of Japanese white oak (*Quercus myrsinaefolia* Bulume) (c) shown as a species with lower conductance in Fig. 6. This result means that it is possible to reliably diagnose slight damage to trees not observed in aerial photographs from the thermal image measured under a cloudy sky above about 300 $\mu\text{mol photon m}^{-2} \text{s}^{-1}$. The surface temperatures of houses (d), roads, and parking lots were above 35°C.

The measured temperature is influenced by absorption and radiation by the atmosphere, although the influence is small in the wavelength range 8 to 13 μm . Figure 8 shows a thermal image, measured from a height of about 700 m, of the same area as that shown in Fig. 7 at about the same time. Points a and d in Fig. 8 correspond to those in Fig. 7B. The leaf temperature measured from ca. 700 m showed a reduction of 0.8°C in comparison with that from ca. 300 m. It must be noted that the extent of this reduction is influenced by atmospheric conditions. A rise in height also causes an error according to the spatial averaging shown in Fig. 3. When the temperature of a tree of 3- to 5- m diameter was measured within 5% error, the height of the helicopter is about 300 to 500 m. The error in the tree's temperature measured by the portable thermal camera increases markedly according to the rise in height.

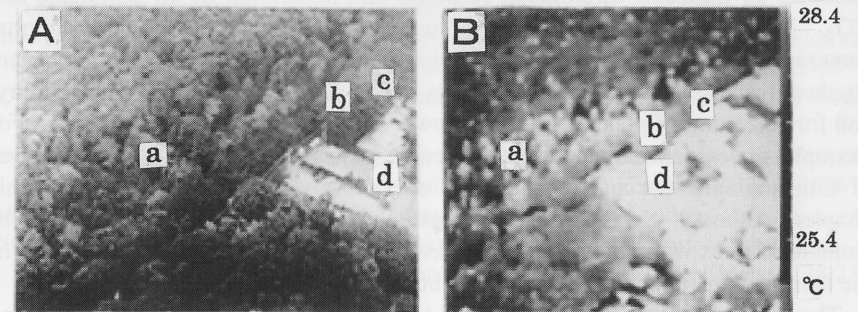


Fig. 7A, B. Aerial photograph (A) and thermal image (B) of temple woods and the adjacent area in the suburbs of Tokyo from a helicopter at a height of about 300 m (Omasa et al. 1993). Sites a to d in A correspond to those in B. Environmental conditions were not measured at the temple, but at a position about 10 km from it; air temperature and PPFD measured after 30 min were about 29°C and 400 $\mu\text{mol photon m}^{-2} \text{s}^{-1}$, respectively

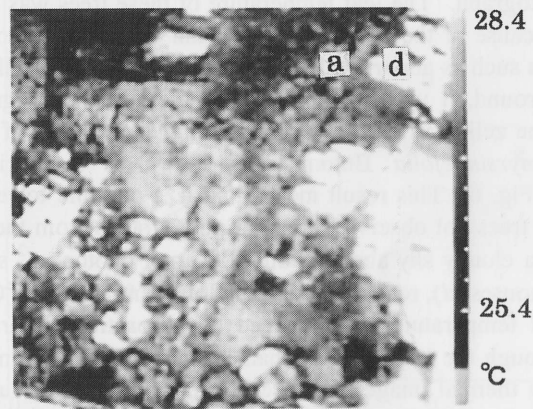


Fig. 8. Thermal image of temple woods and the adjacent area measured from a helicopter at a height of about 700 m (Omasa et al. 1993). Sites *a* and *d* in Fig. 8 correspond to those in Fig. 7. This image was taken at about 100 s before the measurement for Fig. 7

5. Conclusion

Changes in leaf temperature depend on those in transpiration rate from the leaf via stomata under constant thermal conditions; consequently, the leaf temperature becomes an indicator of stomatal response and absorption of air pollutants and CO₂. Therefore, the measurement of leaf temperature by the portable thermal camera can remotely provide spatial information for early detection of plant stresses, because stomatal closure occurs before the appearance of visible injury, and for screening of plants with high growth and high levels of air pollutants. For example, the evidence of spatially different responses of stomata in attached leaves of Chinese laurestine and Japanese red cedar to O₃ exposure was shown in this chapter. Although it was difficult to measure spatial differences in the response of stomata of trees with attached needle leaves using ordinary porometers, the use of the thermal camera made it possible to obtain such spatial information easily.

The thermal camera was also applied to the diagnosis of zelkova trees growing in an urban street and of some species in urban temple woods from the ground and from a helicopter. It was possible to diagnose reliably slight damage to trees that was not observed in photographs from the thermal image measured under a cloudy sky above approximately 300 μmol photon m⁻² s⁻¹. It was necessary to measure at a height less than 300 to 500 m for remote sensing from helicopter to obtain the exact temperature of individual trees.

Recent advance in development of thermal array sensors is remarkable. Consequently, more small-sized, convenient thermal camera with an array sensor such as uncooled FPA are appearing in the market. In the near future, we may easily come to use it like an ordinary video camera.

References

- Colwell RN (ed) (1983) Manual of remote sensing, 2nd edn, vols I, II. American Society of Photogrammetry, Falls Church, VA
- Cowling EB (1989) Recent changes in chemical climate and related effects on forests in North America and Europe. *Ambio* 18:167-171
- Daley PF, Raschke K, Ball JT, et al (1989) Topography of photosynthetic activity in leaves obtained from video images of chlorophyll fluorescence. *Plant Physiol* 90:1233-1238
- Environment Agency of Japan (1991-1993) Global environment research in 1990-1992. C1-C3
- Fuchs M, Tanner CB (1966) Infrared thermometry of vegetation. *Agron J* 58:597-601
- Gates DM, Keegan HJ, Schleter JC, et al (1965) Spectral properties of plants. *Appl Opt* 4:11-20
- Guderian R (ed) (1985) Air pollution by photochemical oxidants: formation, transport, control, and effects on plants. *Ecological studies*, vol 52. Springer, Berlin
- Hashimoto Y, Ino T, Kramer PJ, et al (1984) Dynamic analysis of water stress of sunflower leaves by means of a thermal image processing system. *Plant Physiol* 76:266-269
- Hashimoto Y, Kramer PJ, Nonami H, et al (eds) (1990): Measurement techniques in plant science. Academic Press, San Diego, pp 343-431
- Hobbs RJ, Mooney HA (eds) (1990) Remote sensing of biosphere functioning. *Ecological studies*, vol 79. Springer, New York
- Horler DNH, Barber J, Barringer AR (1980) Effects of cadmium and copper treatments and water stress on the thermal emission from peas (*Pisum sativum* L.): controlled environment experiments. *Remote Sens Environ* 10:191-199
- Inoue Y, Kimball BA, Jackson RD, et al (1990) Remote estimation of leaf transpiration rate and stomatal resistance based on infrared thermometry. *Agric For Meteorol* 51:21-33
- Jones HG (1992) Plants and microclimate, 2nd edn. Cambridge University Press, Cambridge
- Jones HG (1999) Use of thermography for quantitative studies of spatial and temporal variation of stomatal conductance over leaf surface. *Plant Cell Environ* 22:1043-1055
- Monteith JL (1973) Principles of environmental physics. Arnold, London
- Nemani RR, Running SW (1989) Estimation of regional surface resistance to evapotranspiration from NDVI and thermal-IR AVHRR data. *J Appl Meteorol* 28:276-284
- Omasa K (1979) Sorption of air pollutants by plant communities. Analysis and modelling of phenomena (in Japanese). *Res Rep Natl Inst Environ Stud Jpn* 10:367-385
- Omasa K (1990a) Image instrumentation methods of plant analysis. In: Linskens HF, Jackson JF (eds) *Modern methods of plant analysis*. New series 11. Springer, Berlin, pp 203-243
- Omasa K (1990b) Image analysis of chlorophyll fluorescence in leaves. In: Hashimoto Y, Kramer PJ, Nonami H, et al (eds) *Measurement techniques in plant science*. Academic

- Press, San Diego. pp 387-401
- Omasa K (1994) Diagnosis of trees by portable thermographic system. In: Kuttler W, Jochimsen M (eds) Immissionsökologische Forschung im Wandel der Zeit. Essener Ökologische Schriften, pp 141-152
- Omasa K (1996) Image instrumentation of living plants (in Japanese). *Biosci Ind.* 54:545-546, 569-571.
- Omasa K (2000) Phytobiological IT in agricultural engineering. Proc the XIV Memorial CIGR World Congress 2000. pp 125-132
- Omasa K, Aiga I (1987) Environmental measurement: Image instrumentation for evaluating pollution effects on plants. In: Singh MG (ed) Systems and control encyclopedia. Pergamon Press, Oxford, pp 1516-1522
- Omasa K, Croxdale JG (1992) Image analysis of stomatal movements and gas exchange. In: Häder DP (ed) Image analysis in biology, CRC Press, Boca Raton, pp 171-197
- Omasa K, Abo F, Hashimoto Y, et al (1979) Measurement of the thermal pattern of plant leaves under fumigation with air pollutant. *Res Rep Natl Inst Environ Stud Jpn* 10:259-267 (in Japanese and English summary); 11:239-247(1980) (in English translation)
- Omasa K, Abo F, Aiga I, et al (1981a) Image instrumentation of plants exposed to air pollutants: quantification of physiological information included in thermal infrared images. *Trans Soc Instrum Control Eng.* 17:657-663 (in Japanese and English summary); *Res Rep Natl Inst Environ Stud Jpn.* 66:69-79 (1984) (in English translation)
- Omasa K, Hashimoto Y, Aiga I (1981b) A quantitative analysis of the relationships between SO₂ or NO₂ sorption and their acute effects on plant leaves using image instrumentation. *Environ Control Biol* 19:59-67
- Omasa K, Hashimoto Y, Aiga I (1981c) A quantitative analysis of the relationships between O₃ sorption and its acute effects on plant leaves using image instrumentation. *Environ Control Biol* 19:85-92
- Omasa K, Shimazaki K, Aiga I, et al (1987) Image analysis of chlorophyll fluorescence transients for diagnosing the photosynthetic system of attached leaves. *Plant Physiol* 84:748-752
- Omasa K, Tajima A, Miyasaka K (1990) Diagnosis of street trees by thermography. Zelkova trees in Sendai City (in Japanese and English summary). *J Agric Meteorol* 45:271-275
- Omasa K, Shimizu H, Ogawa K, et al (1993) Diagnosis of trees from helicopter by thermographic system (in Japanese and English summary). *Environ Control Biol* 31:161-168
- Omasa K, Kai H, Taoda Z, et al (eds) (1996) Climate change and plants in East Asia. Springer, Tokyo
- Osmond CB, Dayley PF, Badger MR, et al (1998) Chlorophyll fluorescence quenching during photosynthetic induction in leaves of *Abutilon striatum* disks. Infected with abutilon mosaic virus, observed with a field-portable imaging system. *Bot Acta* 111:390-397
- Paoletti E (ed) (1998) Stress factors and air pollution. *Chemosphere* 36:625-1166
- Rencz AN (ed) (1999) Manual of remote sensing, 3rd edn, Vol 3. Wiley, New York
- Sakai A, Larcher W (1987) Frost survival of plants. Springer, Berlin
- Sandermann H, Wellburn AR, Heath RL (eds) (1997) Forest decline and ozone. Springer, Berlin
- Schulze E-D, Lange OL, Oren R (eds) (1989) Forest decline and air pollution. Ecological studies, vol 77. Springer, Berlin

- Schurer K (1975) Thermography in agricultural engineering. Proc. 1st Eur. Congr. Thermography 1994, *Bibl Radiol* No. 6, pp 249-254
- Shimizu H, Fujinuma Y, Kubota K, et al (1993) Effects of low concentrations of ozone (O₃) on the growth of several woody plants. *J Agric Meteorol* 48:723-726
- Taconet O, Olioso A, Ben Mehrez M, et al (1995) Seasonal estimation of evaporation and stomatal conductance over a soybean field using surface IR temperatures. *Agric For Meteorol* 73:321-337
- Waring RH, Running SW (1998) Forest ecosystems: analysis at multiple scales. Academic Press, San Diego